A FULL-HEIGHT WAVEGUIDE TO THIN-FILM MICROSTRIP TRANSITION WITH EXCEPTIONAL RF BANDWIDTH AND COUPLING EFFICIENCY

J. W. Kooi[1], G. Chattopadhyay[1], S. Withington[2], F. Rice[1], J. Zmuidzinas[1], C. Walker[3], and G. Yassin[2]

[1]California Institute of Technology,
MS 320-47 Pasadena, California 91125, USA.
[2]University of Cambridge, Dept. of Physics, UK.
[3]University of Arizona, Dept. of Astronomy, USA.

Abstract

We describe a waveguide to thin-film microstrip transition for high-performance submillimetre wave and teraherz applications. The proposed constant-radius probe couples thin-film microstrip line, to full-height rectangular waveguide with better than 99% efficiency (VSWR $\leq$ 1.20) and 45% fractional bandwidth. Extensive HFSS simulations, backed by scale-model measurements, are presented in the paper. By selecting the substrate material and probe radius, any real impedance between $\approx$ 15-60 Ω can be achieved. The radial probe gives significantly improved performance over other designs discussed in the literature. Although our primary application is submillimetre wave superconducting mixers, we show that membrane techniques should allow broad-band waveguide components to be constructed for the THz frequency range.

Keywords

Radial probe, full-height waveguide to thin-film microstrip transition, suspended membrane, capacitive waveguide tuning step, split-block, hot electron bolometer (HEB), and superconducting-insulating -superconducting (SIS) tunnel junction.

I. Introduction

Many waveguide probe transitions have been proposed over the years, most of which have RF bandwidths of less than 35%. To lower the input impedance, the majority of these designs require significant reductions in waveguide height. Unfortunately, reducing the height makes the machining of THz

components difficult. It also increases RF loss, as the effects of poor surface quality are enhanced by the increased current density in the walls of the waveguide.

At frequencies below 800 GHz heterodyne mixers are typically implemented using waveguide techniques, while above 800 GHz, quasi-optical (open structure) methods are often used. The choice of waveguide offers several advantages over quasi-optical methods, such as the use the ability to use broadband corrugated feed horns with well-defined beam patterns. In practice, however, it has been difficult to couple energy efficiently from waveguide to micron-sized components over a large fractional RF bandwidth. Because nearly all mixer designs have some kind of integrated thin-film tuning structure, there is now a need for an efficient waveguide to thin-film microstrip transition that covers at least one full waveguide band, and is also easily extendible to THz frequencies.

To date, the majority of SIS and HEB waveguide mixers have employed planar probes that extend all the way across the waveguide [1]-[3]. An important reason for the popularity of this kind of design is the convenience with which the active device can be biased and the IF signal extracted. Unfortunately, this kind of "double-sided" (balanced) probe exhibits a rather poor RF bandwidth ($\leq$ 15%) when constructed in full-height waveguide. When the height of the waveguide is reduced by 50%, the probe's fractional bandwidth improves dramatically to a maximum of about 33% [2]. Reducing the height, however, can result in significant fabrication problems (e.g. cost) and increased RF loss, especially at frequencies near or above a terahertz. These results can be understood in that the popular double-sided probe is essentially a planar variation on the well known Eisenhart and Khan waveguide probe [1]. Borrowing from Withington's assessment [4], the real part of the probe's input impedance is influenced in a complex way by the parallel sum of individual non-propagating modal impedances, and as such, is frequency dependent. By reducing the height of the waveguide the ef-

fects of the non-propagating modes can be reduced, which has been done very successfully, for example, by Tong and Blundell *et al.* [2].

An alternative approach is to use an assymetric probe that does not extend all the way across the waveguide. For this kind of probe, referred to from now on as a "one-sided" probe, the modal impedances add in series. The real part of the input impedance only comes from the single propagating mode, and is relatively frequency independent [4]. These probes are typically implemented in full-height waveguide, which minimizes conduction loss and eases fabrication complexity. Though a rectangular version of the "one-sided" probe is used quite extensively by microwave engineers [5], [6] and was introduced to the submillimeter community by Kerr *et al.* [7] in 1990, it is seen to be fundamentally different from the proposed radial-shaped probe.

The radial probe described here represents an attempt to extend the use of radial modes, which are known to give superior broad band performance in thin-film microstrip radial tuning stubs, as compared to rectangular stubs, to the microstrip to waveguide coupling problem. Indeed, by using a spectral-domain method based on numerical Fourier transforms we have shown, in unpublished work, that whereas the transverse component of surface current does not have much influence on the behaviour of rectangular probes, it is central to the operation of radial probes. From a practical point of view, the radial probe can be made, quite naturally, to feed a thin-film microstrip line that has a small line width and thin insulator thickness. In the case of a rectangular probe, there would be a large geometrical discontinuity. Experimentally we have found radial probes, implemented in the described thin-film configuration, to give vastly superior performance over the more traditional approach.

In this paper an effort has been made to understand all aspects of the "one-sided" thin-film radial-probe waveguide transition as applied to substrate and suspended membrane

configurations. The idea is extended from a basic geometry, simply comprising a probe in a waveguide, to more elaborate arrangements, and finally through to practical applications.

Despite various attempts, we have not been able to construct an elegant space or spectral-domain theoretical model of the radial probe. The problem is two-fold: first it is necessary to use an awkward mixture of radial coordinates and Cartesian coordinates, and second, it is vitally important to include transverse as well as longitudinal currents. HFSS 3D electromagnetic field simulations have, however, agreed very well with our experimental measurements (see later), and therefore we used HFSS [8] for all of the work described here. In the simulations, the frequency range is 270-430 GHz, and we have assumed the waveguide to have perfect conductivity, i.e. no loss.

II. The Radial Probe Configuration

In 1999 Withington *et al.* [9] presented an extensive theoretical analysis of a "one-sided" rectangular probe in full-

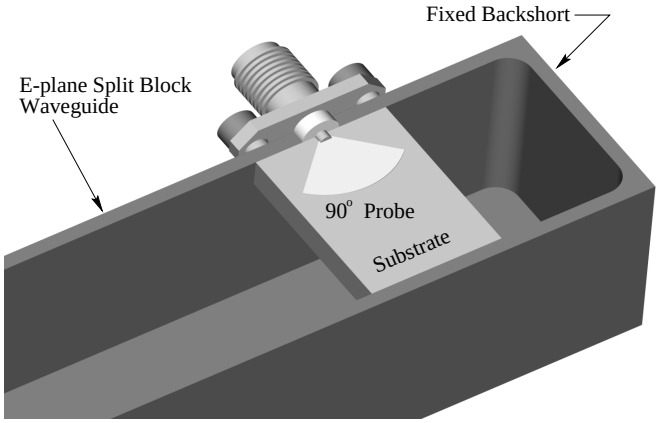

Fig. 1. The probe configuration used in Withington's experiment [4]. The orientation is parallel to the E-field of the TE10 waveguide mode, and in our case in the plane of the split-block. It is possible to rotate the probe by 90° without much change in performance.

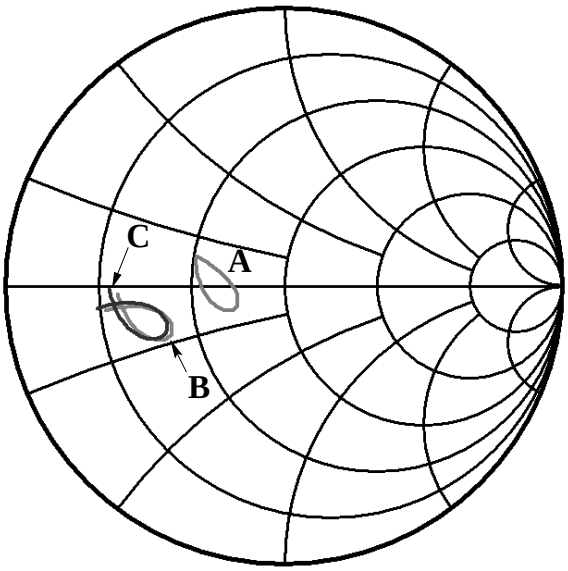

Fig. 2. Simulated input impedance of a 90° radial probe on Quartz (A) , Silicon (B), and GaAs (C) substrates. The substrate is situated inside a 600 μm x 280 μm full height waveguide. The Smith chart is normalized to 50 Ω, and the frequency range of the simulation is 270-430 GHz. Refer to Table I for details.

height waveguide [6], [7]. In his paper, alternative shapes of metallization were investigated, and very promising scale model measurements of a probe with a constant radius were presented. In these measurements a 90° radial fan was connected to a coaxial SMA connector that mounted to the side of split-block waveguide, as shown in Fig. 1. The probe was in the plane of the split block and oriented parallel to the electric field of the waveguide.

Since then, we have used extensive HFSS analyses to extend the idea to include broadband waveguide to thin-film microstrip transitions. In order to minimize fabrication difficulties, we too oriented the probe in the plane of the split-block. Our experience has been that the performance of the probe appears not to be sensitive to its orientation however, and can in fact be rotated by 90° without loss of performance

TABLE I
RADIAL PROBE PARAMETERS OF FIG. 2 AND FIG. 3

Parameter	**Quartz**	**Silicon**	**GaAs**
Dielectric Constant (ϵ_r)	3.78	11.9	12.9
Probe Radius (μm)	112	80	77
Backshort Distance (μm)	77	71	63
Substrate Width (μm)	180	120	120
Substrate Thickness (μm)	50	25	25
Probe Impedance (Ω)	30+j0	17-j6.0	16-j5.5

[13]. Indeed, for free-standing rectangular probes, Withington has shown analytically that the input impedance is only a weak function of orientation [4].

If a coaxial SMA connector were to be connected to a radial probe in full-height waveguide, as in Withington's original experiments, we would measure the input impedance shown in Fig. 2. Several key points should be noted: First, the radius of the probe determines both the RF bandwidth and real part of the input impedance. Optimum bandwidth is always achieved with a frequency dependent "tear drop" shaped input reflection coefficient on the Smith chart. This optimum bandwidth corresponds to a probe radius of 40% of the waveguide height for quartz, and about 30% of the waveguide height for a silicon (Fig. 2 and Fig. 3).

Second, the real part of the probe's input impedance is related to the phase velocity of the launched substrate wave, e.g. proportional to the square root of the dielectric constant. For this particular design of probe, it is of crucial importance that the substrate extends all the way across (or beyond) the waveguide.

Third, the probe's reactance is influenced by the energy stored in the substrate. Changing the height, width, or dielectric constant of the substrate provide convenient and predictable ways to "null" the reactive part of the probe impe-

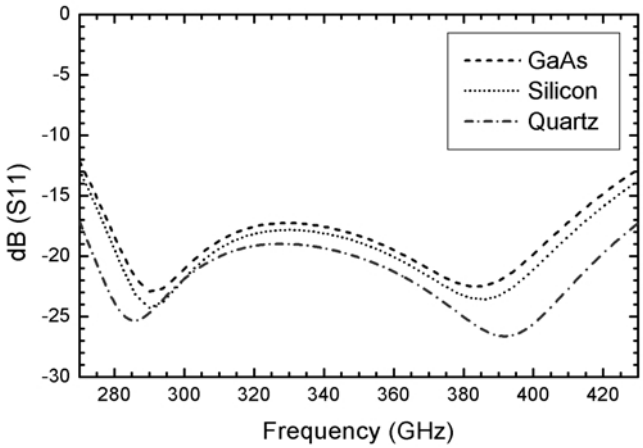

Fig. 3. Input return loss variation of a GaAs, Silicon, and Quartz based radial probe into a fixed load impedance (Table I).

dance. This is demonstrated with the choice of a 50 μm thick quartz substrate in Fig. 2.

Fourth, we found that the real part of the probe's impedance is linearly proportional to the change in opening angle from the 90° reference. In this particular case, the overall RF bandwidth was held fixed (by making small adjustments to the probe's radius).

Finally, it was noticed that the imaginary part of the impedance, to a first order, is proportional to the change in waveguide height. When the waveguide height was reduced by 13%, the imaginary part of the probe's impedance decreased by $\approx 45\%$. These trends are summarised in Table II

TABLE II

Performance trends for radial-probe transitions

$\mathrm{Re}[Z_{probe}]$	$\propto$	Probe Radius, $\epsilon_r^{-\frac{1}{2}}$, $\Delta\theta\vert_{90^\circ}$
$\mathrm{Im}[Z_{probe}]$	$\propto$	Substrate Size, Waveguide height
Bandwidth	$\propto$	Probe Radius

It is worth noting that, if less than the optimum bandwidth is sufficient, the input reflection coefficient can be further improved (S11 $\leq$ -25 dB) by adjusting the radius of the probe (Fig. 6). If both bandwidth and coupling are to be optimized, then a small capacitive tuning step can be used in the waveguide, which we shall discuss in Section VIII.

III. Introduction of a channel into the Waveguide Wall

One of the main aims of this paper is to investigate the efficiency with which radial probes can be used to feed thin-film microstrip lines. In Fig. 4, we show a radial probe with its substrate extending out of the waveguide. In this particular configuration there is a perfect conducting ground plane that extends all the way up to the waveguide wall, which could be achieved in practice by using beam lead contacts along the substrate ground-plane edges. It is vitally important to appreciate, here, that the dielectric supporting the probe is not the dielectric of the thin-film microstrip line.

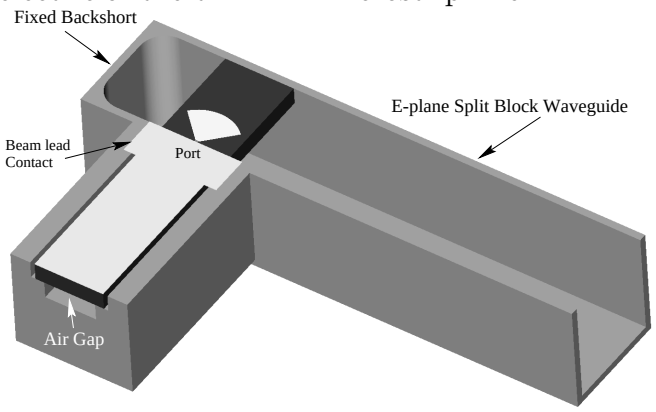

Fig. 4. A transition where the substrate extends out of the waveguide to form a thin-film microstrip circuit. In the simulations, the ratio of air-gap to substrate height is unity. Note that since the backshort position is less than λ_g, the backshort acts as an inductive (shunt) tuning element.

TABLE III
RADIAL PROBE PARAMETERS USED IN FIG. 4 AND FIG. 5

	Wg	**Material**	**Zprobe** Ω	**HU** μm	**Subtrate** μm
A	Yes	Silicon	17-j6	—	25 x 120
B	No	Silicon	22-j3	25	25 x 120
C	Yes	Quartz	30+j0	—	50 x 180
D	No	Quartz	42+j9	50	50 x 180
E	No	Quartz	40+j7	50	50 x 160

"Wg" denotes whether an opening has been made in the wall of the waveguide to accommodate a substrate, HU denotes the air gap underneath the substrate. The silicon-based probe has a radius of 80 μm, whereas the quartz-based probe has a radius of 112 μm.

The whole of the thin-film microstrip line—earth plane, dielectric, and wiring layer—are formed by using thin-film deposition techniques on one side of the probe's dielectric substrate. Indeed, in some of our superconducting submillimetre-wave mixers we have used an "inverted geometry" where the earth plane is the last film to be deposited.

Not surprisingly, creating a large opening in the wall of the waveguide perturbs the electric field distribution in the vicinity of the probe. This affects the probe's input impedance in a significant way, but it does not degrade the extraordinary performance that is available: Fig. 5.

Adding an air gap under the substrate is required in nearly all cases in order to increase the cutoff frequency of the dielectric loaded channel to above the probe's band. To maximize the cutoff frequency of the TE_{10} and TE_{01} modes in the channel, we find that one must typically keep the substrate thickness to channel height ratio of ≤ 0.5, and the substrate thickness to channel width ratio of ≤ 0.4 . As far as the TE_{10} and TE_{01} mode cutoff frequencies of the substrate channel are concerned, the optimal shape appears to be about square. Reducing the width of the bottom air gap by up to 20% to

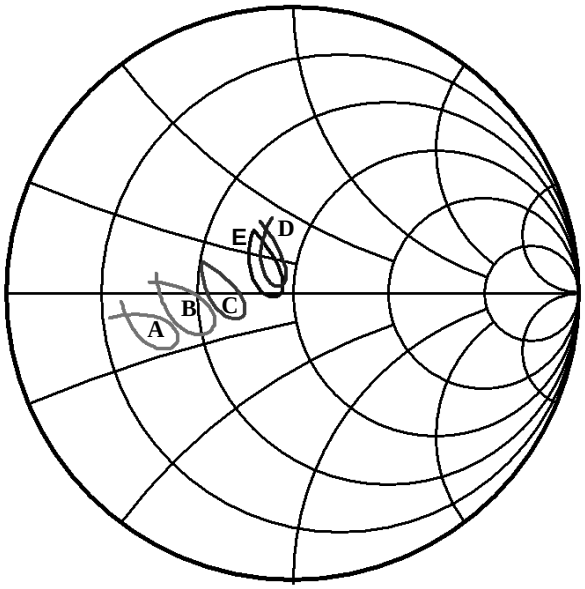

Fig. 5. Progression of impedance circles as a result of adding a channel to the waveguide wall in close proximity to the probe (Fig. 4. Details are listed in Table III.

provide support for the substrate has no significant effect on the performance.

Referring to Fig. 5 and Table III, adding an air channel to the waveguide wall increases the silicon based probe impedance from 17-j6 Ω → 22-j3 Ω (A⇒B). For quartz the impedance is seen to change from 30+j0 Ω → 42+j9 Ω (C⇒D). The RF bandwidth of the probe can easily be reoptimized by a slight adjustment of the probe's radius. In the case of quartz, a 11% decrease of the substrate width (D⇒E) results in a decrease in probe impedance of 42+j9 Ω to 40+j7 Ω.

IV. Probe Impedance as a Function of Radius and Throat Dimension

Apart from knowing the probe's impedance precisely, it important to understand, in general terms, the effect of varying probe and throat radius on bandwidth and RF coupling. We

have defined the probe's throat as being the width of the microstrip line that drives the probe. Simulations indicate that the input impedance and RF bandwidth of the probe is not a sensitive function of the width of the throat, but is sensitive to the probe's radius. Fortunately, the exact probe radius can be precisely set by lithographic means. If maximum bandwidth is not required, it has been observed (Fig. 6) that improved performance over a narrower bandwidth is readily obtained by a slight adjustment of the probe's radius. The throat can be sized to match into any convenient microstrip or coplanar transmission line with no adverse effect on the probe performance. In the simulations, the apex of the 90° probe has been positioned at the edge of the waveguide.

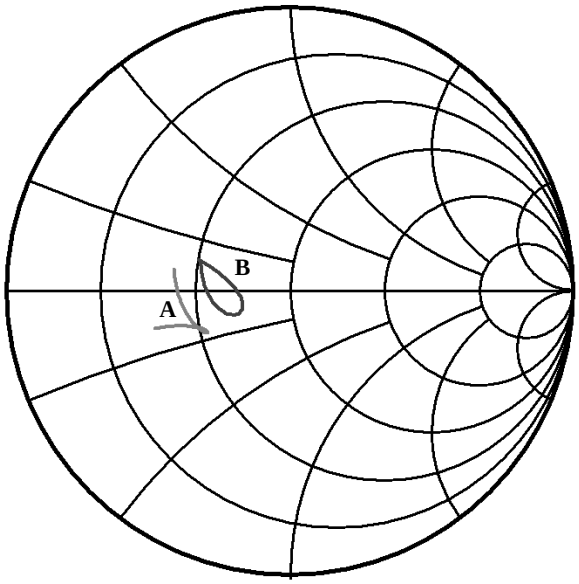

Fig. 6. Impedance sensitivity to probe radius. Reducing the probe's radius by 9% (r=112 μm (B) $\rightarrow$ r=100 μm (A)) lowers the fractional bandwidth from 45 % to 33 %, and the impedance from 30+j0 Ω to 25-j8 Ω). It provides a convenient way of trading off coupling efficiency against bandwidth. Here, the substrate is Quartz (ϵ_r=3.78).

V. Addition of a 4-Section RF choke

Extending the RF ground all the way to the waveguide wall, is in many instances problematic. This is especially the case when operating frequencies approach (or exceed) the terahertz range. Beam-lead techniques (Fig. 4), as are often used in GaAs Schottky diode multiplier processes, and are a viable option [10], [11]. This scheme, however, requires advanced, and therefore expensive processing. Furthermore, the beam-lead process is not readily extendible to quartz substrates, which due to their low (ϵ_r=3.78) dielectric constant and RF loss are often the substrate of choice in the submillimeter wave region. An RF choke in the ground plane may be used to provide a good ground at the waveguide wall (Fig. 7). This idea can be extended to include membranes [12], [13], which offer a good alternative to quartz substrates at frequencies near or above a terahertz (Section VII).

In Fig. 8 we show the progression of the radial probe's input impedance as a 4-section RF choke, with airgaps above and below the substrate, is added. Extending the substrate out of the waveguide in such a manner moves the probe's

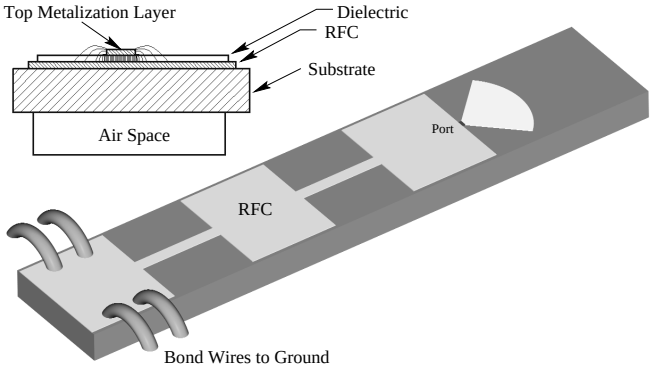

Fig. 7. RF choke providing a ground potential at the waveguide wall. The IF and bias lines run on top of the choke's metalization, which serves as a ground layer for thin-film microstrip or coplanar transmission lines, as shown on the inset (not to scale). The bond wires provide the DC bias return.

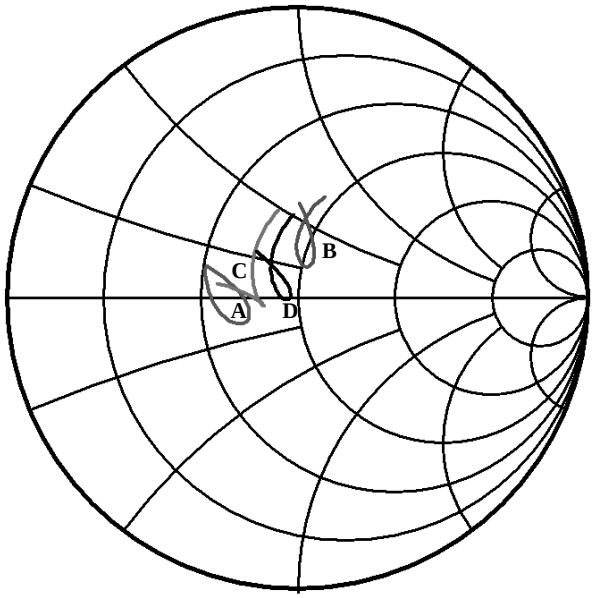

Fig. 8. Progression of probe input impedance as the substrate is extended out of the waveguide (with air on top and bottom) and a 4-section RF choke with ≈35 dB of isolation is added. The bandwidth-limiting effect of the RF Choke can be compensated by increasing the radius of the probe. The substrate material is quartz: details in Table IV.

impedance from 31+j0 Ω to 49+j18 Ω (A ⇒ B). The height of the air gap, directly above the substrate, should be minimized as it can limit the high frequency response of the probe. This is especially relevant if an RF choke is added. The introduction of an RF choke results in a significant and always predictable trend toward lower input impedances (B ⇒ C). The high frequency tail, on the locus of the impedance, is due to evanescent fields directly above the first section of the RF choke. This effect can be mitigated by minimizing the air gap above the substrate.

In the case of the RF choke, a small loss of bandwidth is evident from the Smith chart. If this is a concern, the RF bandwidth can be easily recovered by increasing the probe's

TABLE IV
RADIAL PROBE PARAMETERS USED IN FIG. 8

	Ground	**Radius** μm	**HH** μm	**HU** μm	**Zprobe** Ω
A	Perfect	112	0	0	30+j0
B	Perfect	112	25	50	49+j18
C	RFC	112	25	50	37+j0
D	RFC	122	25	50	43+j6

Ground denotes a perfect (beam-lead) contact up to the waveguide wall. HH denotes the air height above the substrate, HU the air height directly below the substrate

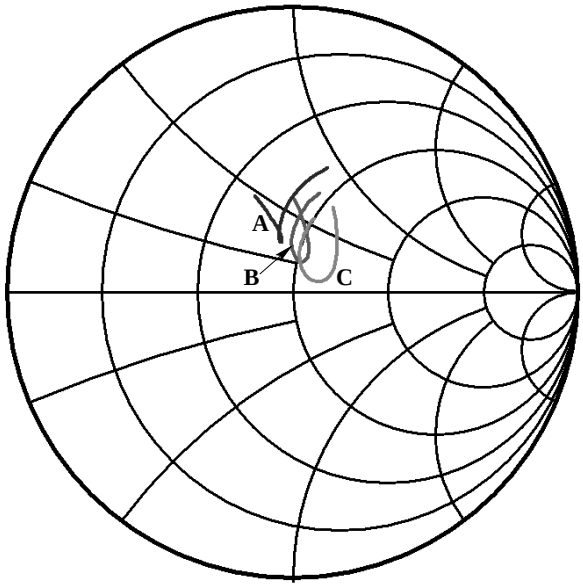

Fig. 9. Progression of probe's input impedance and bandwidth as the substrate (50 μm quartz) is misaligned in the waveguide. "A" is the case of a 4% misalignment outwards from the waveguide, "B" is the perfectly aligned situation, and "C" is the case where the probe is moved 4% into the waveguide. The size of the waveguide is 600 μm x 280 μm.

radius (C $\Rightarrow$ D), and by adding a small capacitive tuning element in the waveguide (section VIII). Also, we have not investigated the effect of using more complicated, broadband filter geometries.

VI. Sensitivity to Probe Misalignment

In general, it is important that the apex of the probe is well aligned with the edge of the substrate ground plane, and that they are both be well aligned with respect to the waveguide wall. In practical systems, however, alignment of the probe cannot be guaranteed. Therefore, we ran a set of simulations to better understand the effect of misalignment. As can be observed from Fig. 9, misalignment of the probe essentially varies the "effective" radius of the probe, thereby altering the shape (bandwidth) of the probe's response. Misalignment errors should be kept less than 3-4% of the waveguide height. If a channel is cut into the opposite waveguide wall, the substrate can then be manually aligned to accommodate dicing errors, ensuring at the same time that the substrate extends across the waveguide.

VII. Radial Probe configuration on a Suspended Membrane

As the frequency of operation exceeds $\approx$ 1 THz, conventional techniques such as those described above become problematic, both in terms of waveguide probe implementation and the fabrication of the waveguides themselves. Recent developments in laser micromachining technology now allow successful waveguide designs to be scaled to terahertz frequencies [14]. In this section, we describe how waveguide probes can be implemented in silicon micromachined waveguide structures.

At these high frequencies very small dimensions are required to prevent energy from leaking out of the substrate channel (suspending the substrate helps by reducing the effective dielectric constant, ϵ_{eff}). This makes assembly of the mixer block difficult. To overcome these problems, we pro-

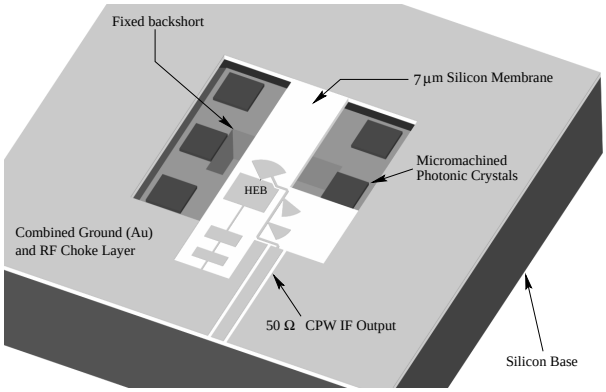

Fig. 10. As an example, we show a radial probe design implemented on 7 μm suspended silicon membrane ($\epsilon_{eff} = 3.216$). Suspending the membrane reduces significantly the sensitivity to height misalignment.

pose the use of a radial probe mounted on a suspended substrate in a full height waveguide. It is found that the combination of a suspended membrane and a radial probe is an especially suitable interface for extremely broadband hot electron bolometers (HEB). It allows HEB's to be integrated with well understood waveguide and feedhorn structures, affording minimal optical loss with well behaved Gaussian beams over extremely large RF bandwidth.

To deal with both phonon and diffusion cooled HEB's, two types of radial-probe, membrane circuits have been designed. The diffusion cooled HEB is mounted on a 1 μm thick silicon-nitride membrane, whereas the phonon cooled HEB is deposited on a somewhat thicker 7 μm membrane. Both membranes are suspended to facilitate simple mounting techniques and reduced sensitivity to height variation. The membranes use silicon as their support base [12], [13], though other materials such as GaAs [15] can be used. To avoid excitation of substrate modes in the membrane it is essential for the 7μm thick silicon membrane, that a substrate channel with a fundamental mode cutoff frequency below that of the highest frequency of operation is formed [15]. Extensive HFSS simula-

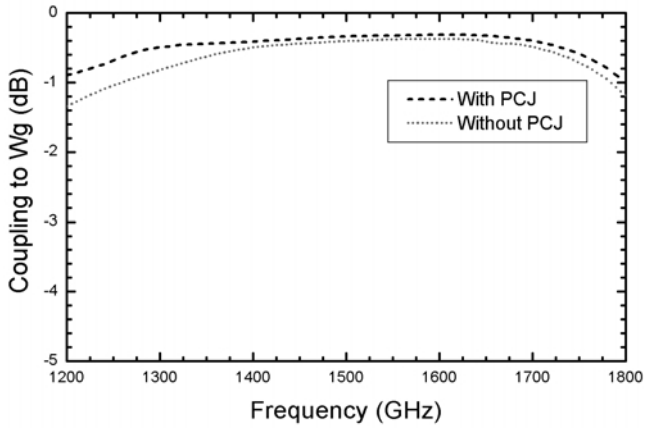

Fig. 11. Simulated coupling efficiency to a full height waveguide horn block for a 50 Ω device (HEB). Photonic crystals serve to scatter the fields in the airgap directly above and below the substrate, thereby reducing RF loss. To get a realistic sense of the loss, all metals except for the waveguide, have been assigned the conductivity of room temperature gold ($4.1*10^7$ S/meter).

tions on a 1μm thick silicon-nitride membrane show that mode free operation to 5.6 THz is achievable. At higher frequencies the silicon nitride membrane thickness should be reduced. As seen in Fig. 10, the IF and bias lines are extracted near the center of the radial probe at a 45° angle. This proved to be the location of minimum perturbation to the surrounding fields (response). The configuration shown is ideal for large-format spectroscopic imaging arrays. The IF and bias lines can then be taken to the edge of the substrate where they are connected to low profile MMIC amplifier chips and bias circuits. Photonic crystal junctions (PCJ's) are used on both top and bottom waveguide blocks [16]. These PCJ's can be thought of as RF chokes, and are an efficient means to scatter the fields improving the RF efficiency by as much a 1 dB. In Fig. 11 we show the waveguide coupling efficiency for a 50 Ohm impedance device with, and without, the use of photonic crystals. Designs such as these, have been submitted for fabrication, and show that radial probes can be combined with

suspended membrane and silicon micromachining techniques to form a whole new generation of circuits for the terahertz frequency range.

VIII. Addition of a Capacitive Tuning Element

If very broadband operation is required, then a dramatic improvement in the probe's performance can be achieved by adding a simple capacitive waveguide tuning step, just in front of the probe. The added capacitive element collapses the characteristic "tear drop" impedance locus into a tiny "star", as shown in Fig. 13.

Fig. 12 shows a diagram of a probe with the waveguide tuning step added. Typically, a 15% reduction in waveguide height is adequate to tune out most of the probe's residual impedance variation. The length of the step is on the order of the height dimension of the waveguide. Because some of the reactance in the probe is tuned out by the step, the distance between the substrate and backshort must be increased

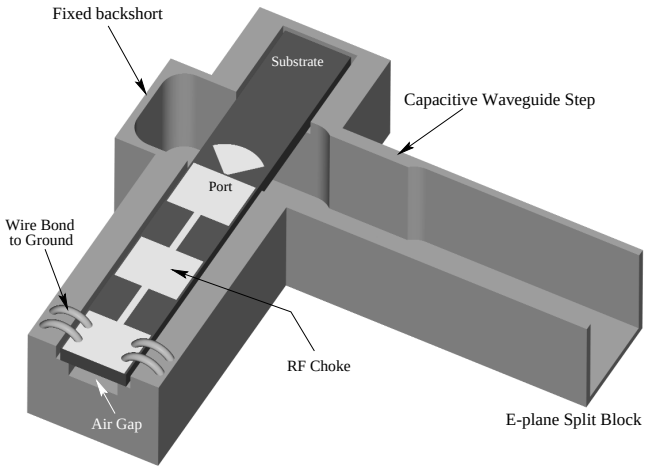

Fig. 12. Inclusion of a capacitive tuning step in front of the radial probe. Though the physical size of the waveguide constriction is small ($\approx$ 15%), the reduction of the probe's input return loss and increase in bandwidth are dramatic.

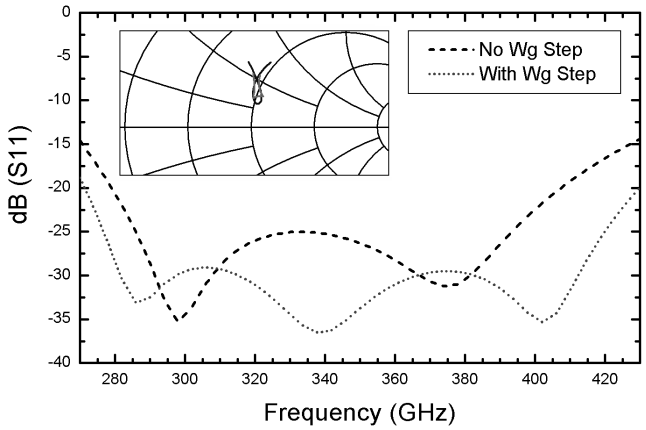

Fig. 13. Input return loss of the radial probe, with and without the capacitive waveguide tuning step. Here a (31 Ω) reference impedance is used, as this is typical of SIS tunnel junction mixers. The characteristic "tear drop" impedance locus of the probe collapses into a "star".

slightly: ($\Delta \approx 0.03$-$0.04\%\ \lambda_g$).
This increase in distance is an additional advantage of using a waveguide step as it actually eases circuit and machining tolerances. Chamfered corners in the waveguide have no effect on the overall performance of the probe, as long as the position of the backshort is compensated for accordingly. The capacitive waveguide step does not affect the impedance locus of the probe.

IX. Scale model Verification

To verify the simulations and obtained results, we ran a series of S-band scale model measurements. The experimental arrangement is shown in Fig. 14. For calibration standards we used 1, 50, and 100 Ohm chip resistors. After making a small adjustment for the physical length of the chip resistors, we established the phase reference at the edge of the waveguide. The substrate material was Stycast with a measured dielectric constant of ϵ_r=4.05 and a loss tangent δ=0.020. In Fig. 15, we present the results which verify the accuracy of the HFSS [8]

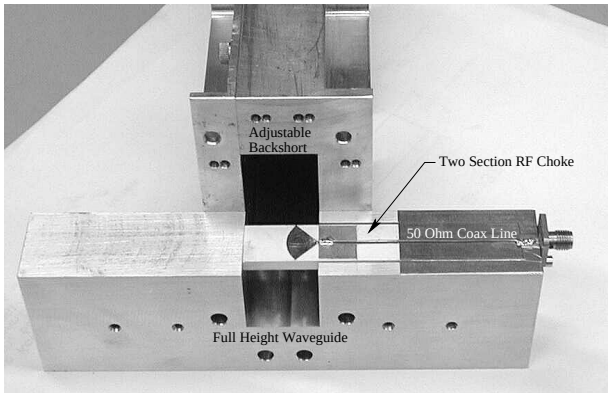

Fig. 14. Scale model (3.4-5.4 GHz) of the radial probe with a 2-section RF choke and capacitive tuning step (not shown). The reference plane for the measurements is at the waveguide wall. The waveguide dimensions are 47.6 x 22.2 mm, the probe radius 9.5 mm, and the Stycast substrate dimensions 13.8 x 4 mm. The substrate height to airgap (below substrate) ratio is half.

computer simulations. The reactive component of the probe's impedance can be reduced by thinning the substrate and/or

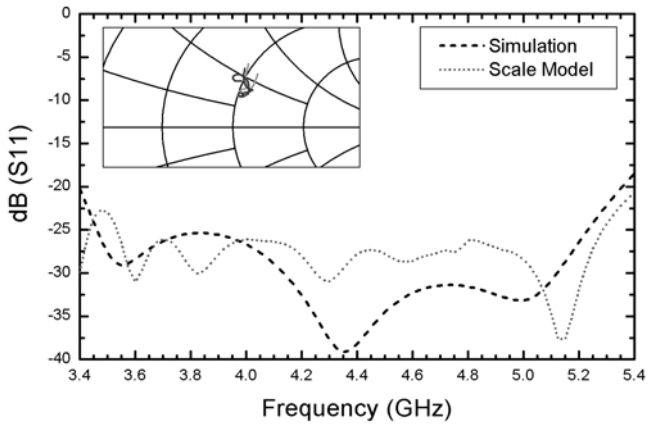

Fig. 15. Measured and simulated return loss to a matched load. The input impedance of the modelled radial probe is 50+j20 Ω. These results include a two section RF choke with a capacitive tuning step in the waveguide.

increasing the airgap under the first section of the RF choke. Based on scale model data, below the cutoff frequency of the waveguide, the radial probe is modeled very precisely as a 7 pF capacitor, normalized to 1 GHz.

X. Example of a fixed-tuned 270-430 GHz design

As a summary of our work, we present, in Fig. 16, a comprehensively modelled design for a 270-430 GHz SIS mixer. The mixer block consists of a full-height, fixed tuned waveguide, which excites a superconducting tunnel junction (SIS) heterodyne detector. The mixer block employs a capacitive tuning step 82 μm in front of the probe, as discussed in Section VIII. A 12-13 % reduction in the height of the waveguide with a length of 240 μm was found to be optimal. The substrate width (200 μm) was dictated by the need to accommodate the 118 μm radial probe. This in turn required the use of an air-gap underneath the substrate, to raise the cutoff frequency of the dielectric-loaded IF channel to above the RF operating frequency range of the receiver.

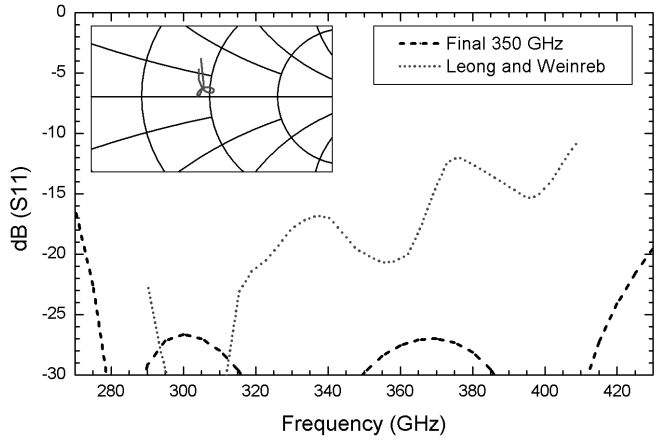

Fig. 16. The predicted input return loss of a fixed tuned full-height SIS mixer block. Also shown is the predicted performance from a rectangular probe reported by Leong and Weinreb *et al.* [6]. The fractional bandwidth of the 350 GHz full height waveguide radial probe is $\approx 45\%$. Refer to Table V and the text for details.

TABLE V
PARAMETERS USED FOR THE 270-430 GHz DESIGN

Parameter	
Substrate material	Quartz
Waveguide size (μm)	600 x 280
Probe radius (μm)	118
Substrate width (μm)	200
Substrate thickness (μm)	50
Air Height above substrate (μm)	25
Air Height below substrate (μm)	50
Backshort distance (μm)	103
Probe impedance (Ω)	47 + j3

XI. CONCLUSION

We have presented and discussed in some detail an inherently low-impedance, broad-band, "one-sided", full-height waveguide to thin-film microstrip transition. Extensive computer simulations suggest that the optimum geometry for this kind of transition is one with constant radius, that is to say a radial fan. It has been shown that the proposed probe couples with better than 99% efficiency over at least a 45% fractional bandwidth. Though the orientation of the probe is not critical, the results presented are solely for a split block design, with the substrate parallel to the split in the block. The combination of full height waveguide, very broad tunerless bandwidth, and thin-film membrane techniques opens up the possibility of using waveguide for making detectors, such as HEB mixers, at frequencies well above 1THz. Simulations and scale model measurements suggest that a small capacitive step in the waveguide is able to tune out most of the residual impedance variation, with frequency, of the probe. Insignificant as the waveguide step may seem, it affords a major improvement in bandwidth and efficiency, while easing

machining and circuit tolerances.

Though the probe has been developed for use with broadband, fixed-tuned SIS and HEB mixers in the submillimeter and THz regions, there are numerous narrow-band and broadband applications at millimeter wavelengths. Examples include compact, low-loss waveguide to coaxial or microstrip transitions, and compact broadband waveguide terminations.

Perhaps one of the most significant features of the radial probe is that by selecting appropriate substrate materials and probe dimensions, any real impedance between $\approx$ 15 and 60 Ω can be achieved.

XII. Acknowledgements

We wish to thank Sander Weinreb of JPL for very helpful discussions on "one-sided" waveguide probes and Mick Edgar of Caltech for many inspirational and stimulating discussions. This work was supported in part by NSF Grant# AST-9980846.

References

[1] R. L. Eisenhart and P. J. Khan, "Theoretical and experimental analyses of a waveguide mounting structure", *IEEE, Microwave Theory and Techniques,* Vol MTT-19, pp. 706-717 (1971)

[2] Tong C-Y. E., Blundell R, Paine S, "Design and characterization of a 250-350-GHz fixed-tuned superconductor-insulator-superconductor receiver", *IEEE, Microwave Theory and Techniques,* Vol MTT-44, pp. 1548-1556, Sept. 1996

[3] J. W. Kooi , M. Chan, B. Bumble, and T. G. Phillips, "A low noise 345 GHz waveguide receiver employing a tuned 0.50 μm^2 Nb/AlO_x/Nb tunnel junction," *Int. J. IR and MM Waves,* vol. 15, No. 5, May 1994.

[4] S. Withington, and G. Yassin, "Analytical expression for the input impedance of a microstrip probe in waveguide," newblock*Int. J. IR and MM Waves,* Vol. 17, pp. 1685-1705, Nov. 1996.

[5] Y-C Leong, and S. Weinreb "Full-band Waveguide-to-microstrip probe transitions" *IEEE, Microwave Theory and Techniques,* Digest of Papers, Anaheim, CA, June 13-19, 1999.

[6] J.H.C. van Heuven "A new integrated waveguide-microstrip transition", *IEEE, Microwave Theory and Techniques,* Vol MTT-24, pp. 144-147, March 1976

[7] A. R. Kerr and S. K Pan, "Some recent developments in the design of SIS mixers,", *Int. J. IR and MM Waves,* Vol. 11, No. 10, pp. 1169-1187, Nov. 1990.

[8] Ansoft Corporation Four Station Square, Suite 200, Pittsburgh, PA 15219-1119, USA

[9] S. Withington, G. Yassin, J. Leech, and K. G. Isaak, "An accurate expression for the input impedance of one-sided microstrip probes in waveguide", *Tenth International Symposium on Space Terahertz Technology,* Charlottesville, March 1999

[10] E. Schelecht, G. Chattopadhyay, A. Maestrini, A. Fung, S. Martin, D. Pukala, J. Bruston, and I. Mehdi, "200, 400, and 800 GHz Schottky diode substrateless multipliers: Design and Results," *2001 IEEE, MTT-S International Microwave Symp. Digest,* Phoenix, Az, pp. 1649-1652, May 2001.

[11] G. Chattopadhyay, E. Schlecht, J. Gill, S. Martin, A. Maestrini, D. Pukala, F. Maiwald, and I. Mehdi, "A Broadband 800 GHz Schottky Balanced Doubler," *IEEE Microwave and Wireless Components Letters,* vol. 12, no. 4, pp. 117-118, April 2002.

[12] J.W. Kooi, J. Pety, B. Bumble, C.K. Walker, H.G. LeDuc, P.L. Schaffer, and T.G. Phillips, "A 850 GHz Waveguide Receiver employing a Niobium SIS Junction Fabricated on a 1μm Si_3N_4 Membrane," *IEEE Transactions on Microwave Theory and Techniques,* Vol. 46, No. 2, pp. 151-161, February 1998.

[13] J. W. Kooi, C.K. Walker, J. Hesler, "A broadband suspended membrane waveguide to microstrip transition for THz Applications," *9th International Conference on Therahertz Electronics,* University of Virginia, Oct. 15-16, 2001

[14] C. K. Walker, G. Narayanan, H. Knoepfle, J. Capara, J. Glenn, A. Hungerford, T. Bloomstein, S. Palmacci, M. Stern, and J. Curtin, "Laser Micromachining of Silicon: A New Technique for Fabricating High Quality THz Waveguide Components" *Eighth International Symposium on Space THz Technology,* Harvard University, Massachusetts, pp. 358-376, 1997

[15] P.H. Siegel, R.P. Smith, M.C. Gaidis, and S. Martin, "2.5 THz GaAs monolythic membrane-diode mixer," *IEEE, Microwave Theory and Techniques,* Vol MTT-47, pp. 596-604, May, 1999.

[16] J. Hesler "A photonic crystal joint (PCJ) for Metal Waveguides" *Submitted to IEEE, Microwave Theory and Techniques,* March, 2001.